Local Wave Field Synthesis by Temporal Bandlimitation

Gergely Firtha
Dept. of Networked Systems and Services
Budapest University of Technologies and Economics
H-1111 Budapest, Hungary
firtha@hit.bme.hu

Nara Hahn
Institute of Sound and Vibration Research
University of Southampton
Southampton, United Kingdom
nara.hahn@soton.ac.uk

Frank Schultz
Institute of Communications Engineering
University of Rostock
18059 Rostock, Germany
frank.schultz@uni-rostock.de

Péter Fiala
Dept. of Networked Systems and Services
Budapest University of Technologies and Economics
H-1111 Budapest, Hungary
fiala@hit.bme.hu

Abstract—Wave Field Synthesis (WFS) aims at the reproduction of a desired target wavefront by driving an ideally continuous loudspeaker distribution with properly chosen secondary source driving signals. In practical applications, using a discrete set of loudspeakers degrades the accuracy of reproduction heavily due to the violation of the theoretical requirements. As a result, spatial aliasing wavefronts emerge from the individual loudspeaker elements in addition to the intended virtual wavefront, perceived as strong coloration above the so-called spatial aliasing frequency. Local Wave Field Synthesis (LWFS) approaches improve the reproduction accuracy over a limited listening area by allowing stronger artifacts outside the control region. The present contribution discusses a novel LWFS approach, relying on the transformation of spatially defined antialiasing filters into an equivalent temporal filter bank. The resulting antialiased driving functions ensure aliasing-free synthesis at a predefined listening position at the cost of temporally bandlimited sound field at other listening regions. The results of the proposed approach are compared with a recent LWFS approach employing direct spatial bandlimitation.

Index Terms—Wave Field Synthesis, LWFS, Spatial antialiasing

I. INTRODUCTION

The aim of sound field synthesis is to reproduce a virtual target sound field over an extended listening area using a densely spaced loudspeaker arrangement, known as the secondary source distribution (SSD). By feeding the loudspeakers with specific driving functions, the superposition of sound fields from each SSD element should ideally match the target sound field in the intended receiving area. One prominent sound field synthesis method is Wave Field Synthesis (WFS) [1], [2].

As WFS obtains the necessary driving functions from a suitable boundary integral representation of the target sound

field, perfect phase correct field-reconstruction could be only achieved by employing a theoretical, continuous secondary source distribution. In practical applications the SSD consist of discrete loudspeaker elements, resulting in secondary wavefronts additionally to the intended virtual wavefront, emerging from the individual SSD elements, termed as aliasing waves. This spatial aliasing phenomenon is perceived as coloration of the synthesized sound field above the spatial aliasing frequency, varying with the listening position and the virtual wavefront direction, degrading the quality of reproduction [3], [4].

The effect of aliasing can be mitigated by restricting the synthesis to a smaller control region inside the listening area at the cost of permitting stronger aliasing artifacts outside the region of interest. These anti-aliased WFS approaches are commonly referred to as Local Wave Field Synthesis (LWFS). Recently introduced LWFS approaches achieve increased local synthesis accuracy by the direct spatial bandlimitation of the WFS driving functions [5]–[8]. However, due to the high computational demand the real-time application of these LWFS approaches is not straightforward.

The present contribution introduces a novel LWFS approach, relying merely on the temporal bandlimitation of the SSD driving functions. The temporal filters, defined uniquely for each SSD elements, are obtained from spatial antialiasing filters by means of an analytical spatial-to-temporal filter transformation, introduced by the current authors in a previous contribution [9]. Similarly to other LWFS techniques, the presented approach ensures aliasing-free synthesis at a predefined listening position at the cost of temporally bandlimited sound field at other listening regions. The results of the proposed approach are compared with a recent LWFS approach employing direct spatial bandlimitation.

The paper is organized as follows: Section II gives a brief theoretical introduction on basic WFS theory and spatial aliasing phenomena. Section III first discusses the spatial-to-

temporal filter transform, then introduces the novel local WFS methodology. Section IV gives a comparison of the presented technique with a recent LWFS approach based on direct modal bandlimitation, followed by a short summary and outlook in Section V.

II. THEORETICAL BASICS

A. Local propagation vector concept

Consider an arbitrary steady-state free space sound field at an angular frequency ω. As a standard ansatz in the field of geometrical acoustics the sound field at a spatial position $\mathbf{x} = [x\,y\,z]^{\mathrm{T}}$ is written in the general polar from as

$$P(\mathbf{x}, \omega) = A(\mathbf{x})\mathrm{e}^{-\mathrm{j}\omega\tau(\mathbf{x})}, \qquad (1)$$

where $A(\mathbf{x})$ and $\tau(\mathbf{x})$ are real-valued functions. This formulation applies to both plane waves and (3D) point sources. The propagation dynamics of the sound field are governed by its phase function $\tau(\mathbf{x})$, termed as the eikonal in the field of ray acoustics [10]. In the temporal domain, the sound field can be obtained by taking the inverse temporal Fourier-transform of (1), yielding

$$p(\mathbf{x}, t) = A(\mathbf{x})\,\delta(t - \tau(\mathbf{x})). \qquad (2)$$

From the above formulation it is evident that the eikonal $\tau(\mathbf{x})$ describes the propagation delay, the wavefront takes to arrive at $\mathbf{x}$. The eikonal equation is obtained by substituting the ansatz (1) into the Helmholtz equation, stating that in a source free volume

$$|\nabla\tau(\mathbf{x})| = \frac{1}{c} \qquad (3)$$

is fulfilled. The gradient of the eikonal weighted by the speed of sound is termed as the local propagation vector

$$c\nabla\tau(\mathbf{x}, \omega) = \hat{\mathbf{k}}^P(\mathbf{x}) = [\hat{k}_x^P(\mathbf{x}),\ \hat{k}_y^P(\mathbf{x}),\ \hat{k}_z^P(\mathbf{x})]^{\mathrm{T}}. \qquad (4)$$

In steady-state, the local propagation vector is perpendicular to the wavefront (equiphase positions) at an arbitrary location of unit length pointing towards the local propagation direction [11]. In the temporal domain it points into the local propagation direction at the time instant of the wavefront passby.

B. 2.5D Wave Field Synthesis

Consider a smooth convex secondary source distribution located at $\mathbf{x}_0 = [x_0,\ y_0,\ 0]^{\mathrm{T}}$ consisting of a continuous distribution of 3D point sources, described by the 3D freefield Green's function, reading in the frequency domain as

$$G_{\mathrm{3D}}(\mathbf{x}, \mathbf{x}_0, \omega) = \frac{1}{4\pi}\frac{\mathrm{e}^{-\mathrm{j}\frac{\omega}{c}\|\mathbf{x}-\mathbf{x}_0\|}}{\|\,\mathbf{x}-\mathbf{x}_0\,\|}, \qquad (5)$$

where ω denotes the angular frequency. In this geometry the target field inside the area bounded by the SSD is described by the Kirchhoff approximation of 2.5D Kirchhoff-Helmholtz integral, from which the 2.5D driving functions can be extracted [12]. For an arbitrary, simple target virtual sound field $P(\mathbf{x}_0, \omega)$ the steady-state driving functions read as [11]

$$D(\mathbf{x}_0, \omega) = \underbrace{\sqrt{8\pi\frac{\mathrm{j}\omega}{c}}}_{H_{\mathrm{pre}}(\omega)}\,w(\mathbf{x}_0)\,\sqrt{d_{\mathrm{ref}}(\mathbf{x}_0)}P(\mathbf{x}_0, \omega). \qquad (6)$$

The driving function consists of
- a frequency dependent pre-equalization filter $H_{\mathrm{pre}}(\omega)$ [1], [2], [12],
- a secondary source selection window [13], [14]

$$w(\mathbf{x}_0) = \max\left(\hat{k}_{\mathrm{n}}^P(\mathbf{x}_0), 0\right), \qquad (7)$$

where $\hat{k}_{\mathrm{n}}^P(\mathbf{x}_0)$ is the normal component of the local propagation vector (i.e. its projection to the SSD normal vector at $\mathbf{x}_0$),
- a gain factor $\sqrt{d_{\mathrm{ref}}(\mathbf{x}_0)}$ allowing amplitude correction along a reference curve, depending on the actual virtual field model (cf. [2], [11]),
- and the virtual field measured on the SSD.

Assuming a simple virtual sound field as given by (1) the driving functions can be written as

$$D(\mathbf{x}_0, \omega) = H_{\mathrm{pre}}(\omega)\underbrace{w(\mathbf{x}_0)\,\sqrt{d_{\mathrm{ref}}(\mathbf{x}_0)}\,A(\mathbf{x}_0)}_{A^D(\mathbf{x}_0)}\mathrm{e}^{-\mathrm{j}\omega\tau(\mathbf{x}_0)}, \qquad (8)$$

and in the time domain as

$$d(\mathbf{x}_0, t) = h_{\mathrm{pre}}(t) *_t A^D(\mathbf{x}_0)\,\delta(t - \tau(\mathbf{x}_0)), \qquad (9)$$

with $A^D(\mathbf{x}_0)$ being the real valued overall gain factor of the driving function, $*_t$ denoting temporal convolution and $h_{\mathrm{pre}}(t)$ is the temporal WFS prefilter impulse response. The analytical, continuous pre-equalization filter impulse response is given in [15], [16], while for an ideal, non-casual FIR filter implementation the reader is referred to [17]. In the following due to the associativity of convolution this prefiltering is excluded from a more convenient discussion.

C. Aliasing artifacts in WFS

The backbone of WFS theory assumes a continuous secondary source distribution. In practical applications the SSD is composed of evenly spaced discrete source elements. As a result, aliasing wavefronts emerge from the individual secondary sources, following the intended virtual wavefront, leading to spatial aliasing phenomena. Although localization does not degrade due to the precedence effect, aliasing is perceived as strong coloration predominantly in the high-frequency region varying with the receiver position and the virtual source position/direction, occurring predominantly above the aliasing frequency.

Figure 1 illustrates spatial aliasing in the temporal domain through the example of the synthesis of an impulsive plane wave, arriving from $\phi_{\mathrm{PW}} = 0°$, applying a discrete secondary source distribution in comparison with a quasi-continuous synthesis scenario. In the current example a circular SSD is applied with the radius of $R_0 = 2$ m, consisting of $N_0 = 90$ 3D point sources. The aliased synthesis in the temporal domain is depicted in Figure 1 (b).

Mathematically, aliasing can be modeled as the discretization of the theoretically continuous driving functions. Assume that a suitable parametrization $d(s, t)$ of the secondary source is given, e.g. the arc length $s = R_0 \cos\phi$ in case of a circular SSD (where ϕ is the polar angle), or the linear position on
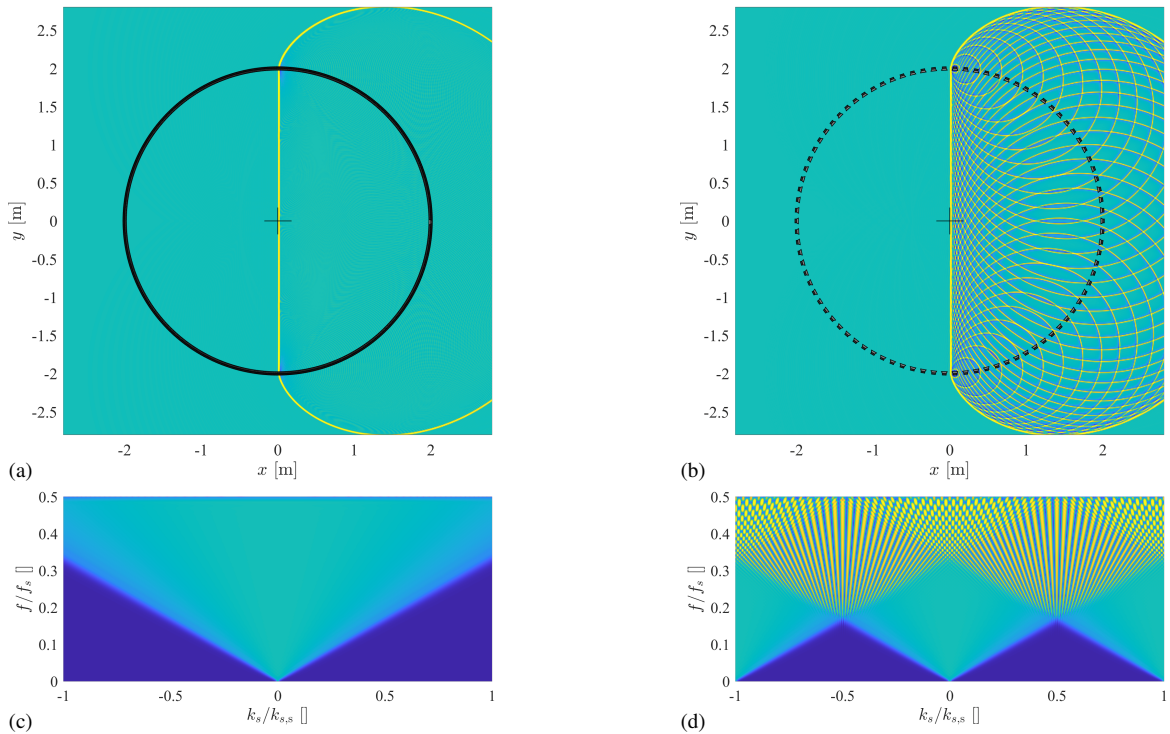
Figure 1. The synthesized field (top) and the spatial spectrum (bottom) of the driving function in case of ideal, quasi-continuous SSD (a) and (c), and in case of a discretized SSD (b) and (d). It is important to note that the spatial spectrum depicts only the non-zero Fourier components (i.e. the Fourier-series coefficients) normalized to the sampling wavenumber.

an infinite, linear SSD. The discretization process is modeled by sampling the driving function by a sampling function, consisting of a series of Dirac-deltas, where the impulse occurences match the actual SSD positions:

$$d_s(s,t) = \sum_{\nu=0}^{N_0-1} d(s,t)\,\delta(s - \nu\Delta s)\,\Delta s, \qquad (10)$$

with Δs being the sampling (arc) length.

By investigating the sampling process in the frequency-wavenumber domain, the spectrum of the sampled driving function is given by

$$\tilde{D}_s(k_s, \omega) = \sum_{\nu=-\infty}^{\infty} \tilde{D}\left(k_s - \nu\frac{2\pi}{\Delta s}, \omega\right), \qquad (11)$$

where $t \to \omega$ and $s \to k_s$ are variable pairs for the Fourier-transform. Obviously, for a closed SSD contour (most notably for a circular SSD) the continuous spatial Fourier-transform yields non-zero components at discrete spatial frequencies on the multiples of the spatial wavenumber, i.e. at

$$k_s = \frac{m}{R_0}, \qquad (12)$$

with $m \in \mathbb{Z}$ constituting a Fourier-series.

In the followings the spatial spectrum refers to the distribution of the non-zero wavenumber values, and the corresponding wavenumber refers to the spatial frequency (multiplied by 2π) of the harmonic basis functions, measured along the closed curve. Figure 1 (c) and (d) illustrate the quasi-continuous and the sampled driving function's spectra.

From (11) it can be deduced that due to spatial sampling, the wavenumber content of the driving function is repeated on the multiples of the sampling wavenumber

$$k_{s,\mathrm{s}} = \frac{2\pi}{\Delta s}. \qquad (13)$$

Since the conventional driving functions are not-bandlimited, therefore, the repeating spectra will overlap above the Nyquist wavenumber $k_{s,\mathrm{Nyq}} = \frac{\pi}{\Delta s}$, for which the corresponding angular frequency is the aliasing frequency of the discretization scheme, as depicted in Figure 1 (d).

According to the sampling theorem, spatial aliasing can be avoided by analytically spatial-bandlimiting the driving functions to the Nyquist wavenumber. This can be performed by either spatially filtering the driving functions with an appropriate spatial low-pass filter prior to numerical evaluation, or performing bandlimitation directly in the wavenumber (modal) domain analytically. The latter approach is implemented by [8], and will serve as a reference solution in the following investigation. However, the modal bandlimitation solution is available so far only for plane wave and point source virtual source models—where the driving functions can be derived analytically—, at the cost of increased computational complexity.

In the following an alternative, approximate solution is presented, allowing spatial antialiasing filtering for an arbitrary

virtual source model and arbitrary SSD contour, performed by FIR (finite impulse response) filtering in the temporal domain. The technique relies on an analytic transform of spatially defined antialiasing filters to an equivalent temporal domain filter bank.

III. TIME DOMAIN ANTIALIASING LWFS

A. Spatial to temporal filter transform

First, a general analytical approach is introduced allowing the transform of an arbitrary spatial filter to an equivalent temporal filter set. From herein, subscript x and t distinguishes whether a filter is defined as a spatial or a temporal filter, respectively.

Assume an arbitrary filter impulse response defined in the spatial domain, denoted by $h_x(s)$. Again, s is a suitable parametrization of the SSD contour. The spatially filtered driving function is obtained from the convolution of the conventional driving functions and the filter impulse response along the SSD contour

$$d'_x(s,t) = h_x(s) *_s d(s,t) = \int h_x(s - s_0)\, d(s_0, t)\, \mathrm{d}s_0, \quad (14)$$

where $*_x$ denotes a circular convolution for a convex SSD contour or a linear convolution in case of an infinite, linear SSD.

Let's assume a temporal filter impulse response, defined for each SSD element $h_t(s,t)$. The temporally filtered driving functions are obtained from the temporal convolution of each SSD elements' driving function by the corresponding temporal impulse response

$$d'_t(s,t) = h_t(s,t) *_t d(s,t) = \int_{-\infty}^{\infty} h_t(s, t - t_0)\, d(s, t_0)\, \mathrm{d}t_0. \quad (15)$$

Our aim is to express the temporal filter bank $h_t(s,t)$ in terms of the spatial filter, so that the result of the temporal convolution (15) coincides with the spatial filtering result (14), i.e.

$$d'_x(s,t) = d'_t(s,t) \quad (16)$$

holds.

1) Exact transformation: The following transformation is allowed by the spatio-temporal structures of the driving functions (9), in which the spatial and temporal dimensions are interconnected in the argument of a Dirac-delta, due to the wave propagation characteristics. The main idea of the derivation is that by exploiting the sifting property of the Dirac-delta in the driving functions, both spatial and temporal convolutions (14) and (15) can be evaluated, from which the temporal filter impulse responses can be expressed as the function of the spatial ones. Again, in the following the pre-equalization filter is omitted from discussion, since equalization filtering can be performed following the antialiasing process.

The temporal convolution in (15) can be evaluated by substituting the general WFS driving function (9) and exploiting the sifting property of the Dirac-delta, yielding

$$d'_t(s,t) = A^D(s)\, h_t(s, t - \tau(s)) \quad (17)$$
$$d'_t(s, t + \tau(s)) = A^D(s)\, h_t(s,t), \quad (18)$$

with the second equation obtained by applying the time shift of $\tau(s)$ for the sake of later simplicity.

The shifted spatially filtered driving function reads as

$$d'_x(s, t + \tau(s)) = \int h_x(s - s_0)\, d(s_0, t + \tau(s))\, \mathrm{d}s_0 =$$
$$\int h_x(s - s_0)\, A^D(s_0)\, \delta(s_0, t + (\tau(s) - \tau(s_0)))\, \mathrm{d}s_0. \quad (19)$$

In order to evaluate the spatial convolution the generalized sifting property of the Dirac-delta may be applied [16], [18], which states that

$$\int f(s_0)\delta(g(s_0))\mathrm{d}s_0 = \sum_i \frac{f(s_i)}{|\frac{\partial}{\partial s_0} g(s_0)|_{s=s_i}|}, \quad g(s_i) = 0. \quad (20)$$

In the present problem the zeros of the Dirac's argument are found where

$$\tau(s_i) = t + \tau(s) \quad (21)$$

is satisfied. In the following it is assumed that a single zero s_i exists, satisfying (21). This assumption means that the wavefront arrives at each SSD element at a unique time instant, being strictly true for a virtual plane wave and a linear SSD. The derivative of the phase function is given by

$$\frac{\partial}{\partial s_0} g(s_0) = -\frac{\partial}{\partial s_0} \tau(s_0) = -\frac{\hat{k}_t^P(s_0)}{c}. \quad (22)$$

Here $\hat{k}_t^P(s_0)$ is the tangential component of the local propagation vector, defined as

$$\hat{k}_t^P(s_0) = \mathbf{t}^{\mathrm{T}}(s_0)\hat{\mathbf{k}}^P(s_0), \quad (23)$$

with $\mathbf{t}^{\mathrm{T}}(s_0)$ denoting the unity long tangential vector of the SSD element at position s_0, as illustrated in Figure 2.

With the above assumptions the integral (19) can be evaluated, yielding

$$d'_x(s, t + \tau(s)) = \frac{c}{|\hat{k}_t^P(s_i)|}\, h_x(s - s_i)\, A^D(s_i). \quad (24)$$

Finally, by combining (24) and (18) the resulting general transformation relation between the spatial and temporal filters is given as

$$h_t(s,t) = \frac{A^D(s_i)}{A^D(s)} \frac{c}{|\hat{k}_t^P(s_i)|} h_x(s - s_i), \quad (25)$$
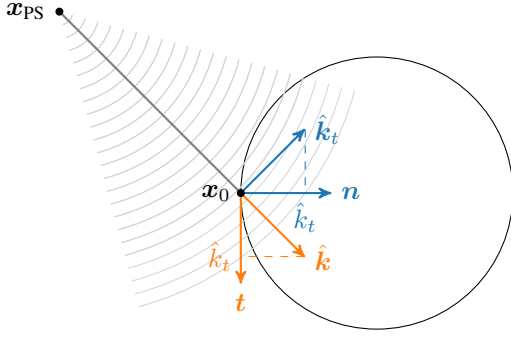
where s_i satisfies (21).

Figure 2. Illustration for the tangential component of the local propagation vector in the exemplary case of the field of a virtual point source, located at $\mathbf{x}_{\mathrm{PS}}$ and applying a circular SSD. On the figure $\boldsymbol{t}$ and $\boldsymbol{n}$ denote the tangential and normal vector of the SSD respectively, $\hat{\boldsymbol{k}}_t$ denotes the tangential vector of the sound sound field and $\hat{k}_t$ denote the tangential component of the local propagation vector ($\hat{\boldsymbol{k}}$) at the SSD position $\mathbf{x}_0$.

2) Local plane wave approximation: The above formulation already allows one to transform an arbitrary spatial impulse response into an equivalent temporal filter for each SSD element, as long as the virtual field model is known and (21) can be solved. In order to give a more general solution it is assumed that the virtual field is locally plane, being a usual high frequency assumption in WFS theory. As a further general WFS assumption it is supposed that the SSD is locally plane. These requirements inherently ensure that a single solution exists for (21)[1]. With these assumptions the phase function is given as

$$\tau(\mathbf{x}) = \frac{\hat{k}_x^P(\mathbf{x})\,x + \hat{k}_y^P(\mathbf{x})\,y}{c} \qquad (26)$$

and (21) is satisfied where

$$s_i = s + \frac{c \cdot t}{\hat{k}_t^P(s)}. \qquad (27)$$

Finally, as a crucial approximation it is assumed that both the amplitude of the driving function and the propagation vector varies slowly along the SSD, i.e $A^D(s_i) \approx A^D(s)$ and $\hat{k}_t^P(s_i) \approx \hat{k}_t^P(s)$ holds. With these assumptions the corresponding filter transform reads as

$$h_t\,(s,t) = \frac{c}{|\hat{k}_t^P(s)|} h_x\left(-t\,\frac{c}{\hat{k}_t^P(s)}\right). \qquad (28)$$

Equation (28) can be directly expressed in the spectral domain by taking the Fourier-transform of both sides, relating the frequency response of the spatial and the temporal filters. By denoting $\mathcal{F}\,(h_x(s)) = H_x(k_s)$ the corresponding transform is given by

$$H_t\,(s,\omega) = H_x\left(-\frac{\omega}{c}\hat{k}_t^P(s)\right) = H_x\left(-k_t^P(s)\right), \qquad (29)$$

[1]Except for a plane wave arriving normally to the SSD, at which case the temporal filter is transformed into a Dirac-delta.

where $k_t^P(s)$ is the tangential component of the local wavenumber vector [2]. Hence, as the main result of the present discussion, the temporal filter transfer can be obtained from the wavenumber (modal) content of the spatial filter by simple rescaling in terms of the local wavenumber vector.

The validity and the error analysis of the above filter transform was investigated in details in [9]. In the following the direct application for local WFS is discussed.

B. Application for antialiasing filtering

Figure 1 (d) reflects that the overlapping of the sampled driving function spectra, and, therefore, the presence of aliasing waves can be avoided by spatially bandlimiting the driving functions to the Nyquist wavenumber prior to sampling. Spatial bandlimitation can be straightforwardly performed by designing a suitable spatial antialiasing filter and transforming it into an equivalent temporal filter bank, based on the results of the previous section. An important advantage of the temporal filtering approach instead of direct spatial filtering is that analyical spatial bandlimitation can be achieved by calculating the WFS driving functions at discrete positions, followed by temporal filtering [3].

Spectral overlapping can be avoided by bandlimiting the driving function to the sampling wavenumber $k_{s,\mathrm{s}} = \frac{2\pi}{\Delta s}$, with either symmetrically to $k_s = 0$ or by choosing an arbitrary central wavenumber $k_{s,0}$. First the former case is investigated in details.

1) Symmetrical antialiasing: As the most straightforward antialiasing strategy, the spectral overlapping is avoided by the spatial lowpass filtering of the driving functions to the Nyquist wavenumber, $k_{s,\mathrm{Nyq}} = \frac{\pi}{\Delta s}$.

The effect of symmetrical bandlimitation is demonstrated via the exemplary low pass filter chosen to be an N-th order Butterworth design, defined in the wavenumber domain as

$$H_x(k_s) = \frac{1}{\sqrt{1 + (k_s/k_{s,\mathrm{Nyq}})^{2N}}}. \qquad (30)$$

From the transform given by (29) the angular frequency response of the equivalent temporal filter bank is given by

$$H_t(s,\omega) = \frac{1}{\sqrt{1 + \left(\frac{\omega}{c}\frac{\hat{k}_t^P(s)}{k_{s,\mathrm{Nyq}}}\right)^{2N}}} = \frac{1}{\sqrt{1 + \left(\frac{\omega}{\omega_c(s)}\right)^{2N}}}. \qquad (31)$$

with

$$\omega_c(s) = c\,\frac{k_{s,\mathrm{Nyq}}}{\hat{k}_t^P(s)} = c\,\frac{\pi}{\Delta s}\,\frac{1}{\hat{k}_t^P(s)}. \qquad (32)$$

Therefore, the cut-off frequency of the equivalent low-pass filter on a given SSD element is inversely proportional to the tangential component of the local propagation vector.

[2]The local wavenumber vector can be defined for a steady state sound field, pointing in the local propagation direction with the length being ω/c [16]

[3]The above statement holds as long as temporally continuous driving functions are assumed. Once the driving functions are sampled with a sampling frequency $f_s = 1/\Delta t$, this corresponds to a spatial sampling prior to the filtering process with $\Delta s = c/f_s$.

The result of antialiasing filtering is depicted in Figure 3 for the synthesis scenario discussed in the foregoing. In the present case the sampling arc length is given by $\Delta s = \frac{2\pi R_0}{N}$, i.e. the space-dependent cut-off frequency reads as

$$\omega_c(s) = \frac{N}{2R_0} \frac{c}{\hat{k}_t^P(s)}. \tag{33}$$

The antialiasing filters are 4-th order Butterworth designs.

Figure 3 (a) shows the result of the synthesis, while Figure 3 (b) illustrates the spectrum of the bandlimited, sampled driving functions. It is highlighted that the presented antialiasing
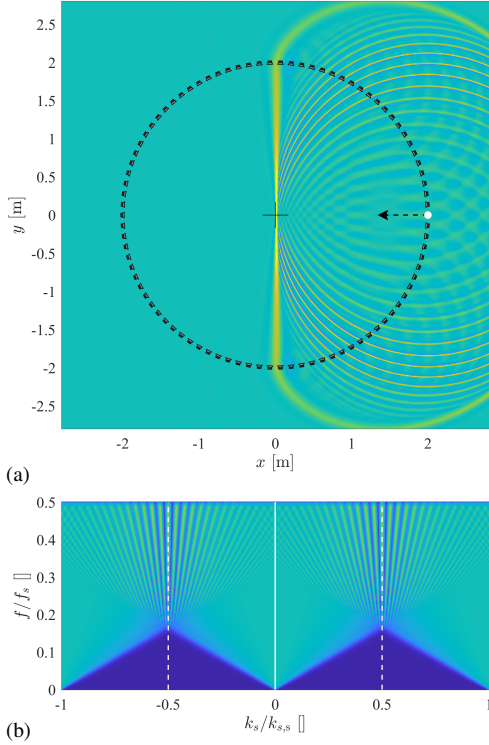

(a)

(b)

Figure 3. Symmetric antialiasing filtering. Figure (a) depicts the synthesized wave front, and (b) illustrates the spatial spectrum of the driving functions.

strategy ensures suppressed aliasing waves in the center of the circular source array. In other positions of the listening area lateral aliasing wavefronts remain in the reproduced wave field, while the target, virtual wave front is bandlimited. This phenomenon can be understood by investigating the synthesis scenario in a geometrical manner:

Since the cutoff frequency of the antialiasing filter (Eq. (32)) is inversely proportional to the tangential component of the virtual field on the SSD, in a circular array a single SSD element will have nearly fullband driving signal: that SSD element at which the wavefront arrives perpendicularly (i.e. where the tangential component of the local propagation vector is zero). This fullband SSD element is marked with white dot in Figure 3 (a). From general WFS theory it is known that the fullband SSD element will dominate the synthesized wavefront (i.e. will serve as a stationary SSD position) for spatial positions along a straight line crossing the actual SSD
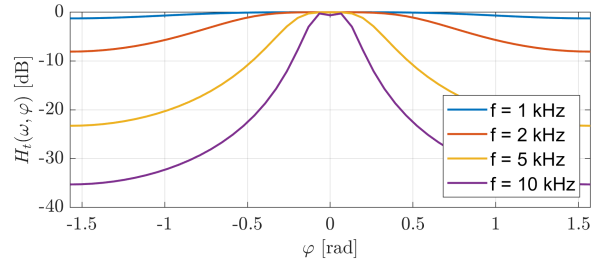

Figure 4. Illustration of equivalent frequency dependent window functions

element into the direction of the local propagation vector [16]. Therefore, the present antialiasing strategy ensures aliasing-free synthesis along a straight line for which the fullband SSD element is the stationary secondary source. The direction of the line of aliasing-free synthesis is marked with a dashed arrow in the figure. This is in contrast with previous LWFS approaches, in which the synthesis is optimized in the proximity of a pre-defined reference position over a circular area.

It should be noted that in the angular, temporal frequency domain the filtered driving function is written as

$$D_t'(s,\omega) = D(s,\omega)H_t(s,\omega) = H_x\left(-k_t^P(s)\right) D(s,\omega), \tag{34}$$

from which formulation it is apparent that in the frequency domain the presented spatial-to-temporal filter transform strategy can be also interpreted as a frequency dependent spatial windowing approach, and the frequency dependent spatial window is given by $H_x\left(-k_t^P(s)\right)$: in the aspect of antialiasing filtering SSD positions where the local tangential wavenumber is higher than the Nyquist wavenumber are highly attenuated, with the window width decreasing with increasing angular frequency. The actual shape of the spatial windows are given by the wavenumber spectrum of the spatial lowpass filter $H_x(k_s)$, rescaled in terms of the local tangential wavenumber. The set of window functions applied in the present simulation scenario are illustrated in Figure 4.

2) Non-symmetrical antialiasing: As an alternative antialiasing strategy, the overlapping of the spectra can be avoided by bandlimiting the driving function spectra with a spatial band-pass filter with an arbitrary center wavenumber $k_{s,0}$ and the bandwidth of the sampling wavenumber $k_{s,s} = 2k_{s,\mathrm{Nyq}}$.

Again, the concept is illustrated via a simple synthesis scenario as discussed in the foregoing. In the present case the spatial bandpass filter is derived by shifting the N-th order low-pass Butterworth design to the a frequency dependent center wavenumber $k_{s,0}(\omega) = \frac{\omega}{c}\hat{k}_{s,0}$ (where $\hat{k}_{s,0}$ is a constant normalized wavenumber value)

$$H_x(k_s,\omega) = \frac{1}{\sqrt{1 + \left(\frac{k_s - k_{s,0}(\omega)}{k_{s,\mathrm{Nyq}}}\right)^{2N}}}. \tag{35}$$

Note, that in this case even the spatial filters are frequency dependent, in order to ensure that the transformed temporal filters remain time-invariant, as explained in the followings.

Again, an equivalent filter bank is derived by using the transform (29), resulting in the frequency response of

$$H_t(s, \omega) = \frac{1}{\sqrt{1 + \left(\frac{\omega}{c} \frac{\hat{k}_t^P(s) - \hat{k}_{s,0}}{k_{s,\text{Nyq}}}\right)^{2N}}} = \frac{1}{\sqrt{1 + \left(\frac{\omega}{\omega_c(s)}\right)^{2N}}},$$

$$(36)$$

with the normalized center wavenumber $\hat{k}_{s,0}$ and with

$$\omega_c(s) = c \frac{k_{s,\text{Nyq}}}{\hat{k}_t^P(s) - \hat{k}_{s,0}} = c \frac{\pi}{\Delta s} \frac{1}{\hat{k}_t^P(s) - \hat{k}_{s,0}}.$$
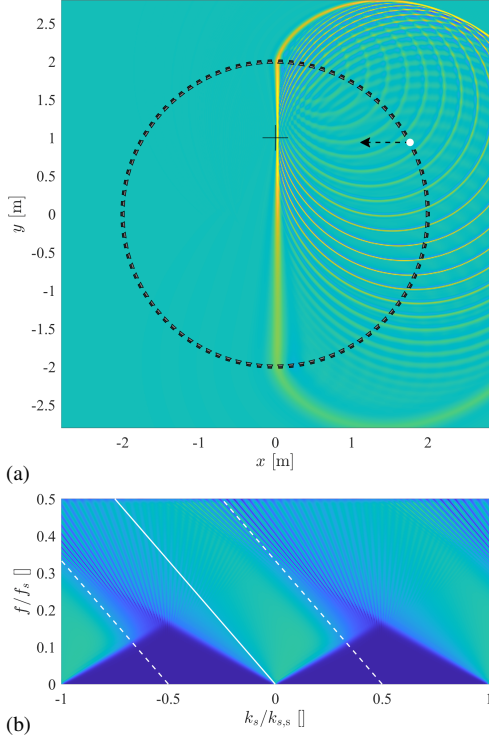
$$(37)$$

(a)

(b)

Figure 5. Non-symmetric antialiasing filtering. Figure (a) depicts the synthesized wave front, and (b) illustrates the spatial spectrum of the driving functions.

The application of the above formulation with an arbitrarily chosen center wavenumber $\hat{k}_{s,0} = 1/2$ is depicted in Figure 5. Note that the wavenumber content of the original spatial lowpass filter is „steered", so that the center frequency varies linearly with the angular frequency and the slope of the variation is given by the normalized center wavenumber. This „steered", frequency dependent band-pass filter theoretically also ensures non-overlapping spectra after the discretization process.

From (37) it is apparent that in the present case the nearly fullband SSD element will be that, where the tangential local propagation vector coincides with the normalized center wavenumber, i.e. where $\hat{k}_t^P(s) = \hat{k}_{s,0} = 1/2$. Again, the fullband SSD element is denoted by white dot in Figure 5 (a). Similarly to the previous case, this fullband SSD element serves as the stationary SSD position for a set of positions located along a straight line passing through the SSD element

with the direction given by this element's local propagation vector. The direction along which fullband synthesis is ensured is denoted by a dashed arrow in Figure 5 (a).

It is important to emphasize that if no actual SSD element exists for a given plane wave direction (for which the wave arrives perpendicularly) then all the SSD elements are bandlimited, i.e. in the synthesized field no fullband synthesis positions will be present. Therefore, for a given receiver position the bandwidth of the reproduced field will depend on the virtual source position/virtual plane wave direction and the loudspeaker spacing. This phenomena will have a clearly audible effect in case of dynamic WFS scenarios (e.g. moving virtual sources) and the possibilities to overcome this limitation is the topic of future research.

3) Application for Local Wave Field Synthesis: The findings of the previous subsections can be straightforwardly used in order to apply the above theory directly for LWFS. In this case a reference position $\mathbf{x}_{\text{ref}}$ is prescribed inside the SSD, at which aliasing-free, amplitude and phase correct synthesis has to be ensured.

Amplitude correct synthesis may be achieved by a suitably chosen reference function in (6), based on the virtual field model. For a detailed treatise on the definition of the reference function the reader is referred to [16].

On the other hand, aliasing components can be suppressed by „steering" the direction of antialiased synthesis to cross the prescribed reference point. This can be performed by finding the stationary position on the SSD for the reference position and choosing the normalized center wavenumber in (37) to coincide with the local propagation vector of the stationary position. Mathematically, this can be formulated as follows. Given a reference position $\mathbf{x}_{\text{ref}}$ and an SSD located along $\mathbf{x}_0$, the stationary SSD element $\mathbf{x}_0^*$ satisfies

$$\frac{\mathbf{x}_{\text{ref}} - \mathbf{x}_0^*}{|\mathbf{x}_{\text{ref}} - \mathbf{x}_0^*|} = \hat{\mathbf{k}}^P(\mathbf{x}_0^*).$$

$$(38)$$

Once $\mathbf{x}_0^*$ is found, the center wavenumber in (37) is found by

$$\hat{k}_{s,0} = \hat{k}_t^P(\mathbf{x}_0^*).$$

$$(39)$$

Obviously, symmetrical antialiasing filtering, depicted in Figure 3 can be regarded as LWFS with choosing $\mathbf{x}_{\text{ref}} = [0, 0]^T$, while Figure 5, illustrating asymmetrical filtering was generated by choosing $\mathbf{x}_{\text{ref}} = [0, 1]^T$. In both cases in Figure 3 and 5 (a) the reference position is denoted by a black cross.

IV. COMPARISON WITH DIRECT MODAL BANDLIMITATION

Finally, the performance of the proposed LWFS approach is compared with conventional a LWFS implementation, based on direct modal bandlimitation [8]. For a direct spatial bandlimitation, the sound field is expanded in terms of cylindrical harmonics with respect to the target position. The modal bandwidth was limited by truncating the expansion to a finite order. Based on the analytical expressions of the modal impulse responses, the LWFS driving functions are implemented as FIR filters in the time domain. The length of the FIR filters depends on the distance between secondary source
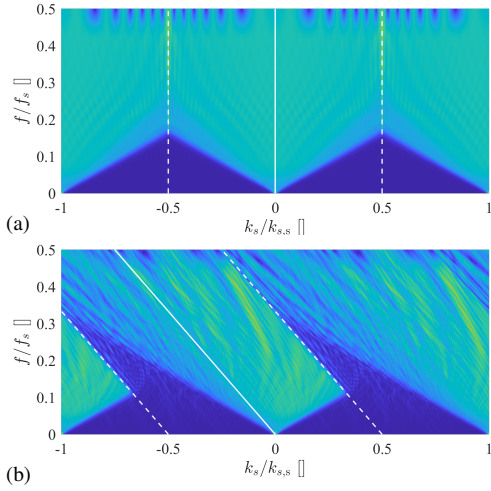
Figure 6. Spectrum of LWFS driving functions by direct modal bandlimitation with the reference position choosen at the center, $\mathbf{x}_{\mathrm{ref}} = [0,0]^{\mathrm{T}}$ (a) and on the left side, $\mathbf{x}_{\mathrm{ref}} = [0,1]^{\mathrm{T}}$ (b).

and the target position, ranging between 273 and 787 taps for the considered scenarios (excluding the WFS prefilter). Since this approach is based on time-domain sampling, the resulting filters exhibit temporal aliasing artifacts, degrading the accuracy in the frequency domain. It is, therefore, crucial to attenuate the spectral components beyond the Nyquist limit before the modal impulse responses are sampled. An analytical anti-aliasing filtering is performed in the continuous-time domain by using the 15th-order Lagrange interpolation kernel. Interested readers are referred to [8] for further detail.

The two methods are compared via the exemplary synthesis scenario discussed in the foregoing, synthesizing an impulsive plane wave, by bandlimiting the driving functions to the Nyquist wavenumber. The result of synthesis is investigated for four different reference positions:

- Center: $\mathbf{x}_{\mathrm{ref}} = [0,0]^{\mathrm{T}}$
- Left: $\mathbf{x}_{\mathrm{ref}} = [0,1]^{\mathrm{T}}$
- Front: $\mathbf{x}_{\mathrm{ref}} = [1,0]^{\mathrm{T}}$
- Back: $\mathbf{x}_{\mathrm{ref}} = [-1,0]^{\mathrm{T}}$

For the central and the left reference positions first the spectra of the driving functions were investigated. Figure 6 already reflects the fact that the proposed temporal LWFS approach is an approximation of the reference solution, i.e. of the direct modal bandlimitation. It is verified that modal bandlimitation LWFS performs the same steering strategy of the modal spectrum into the direction of the central wavenumber, realizing a frequency dependent spatial band-pass filter.

Figure 7 presents the comparison of the two approaches via the synthesized field and the frequency response, each column illustrating a different reference position. The first row (a-d) shows the synthesized field at the time instant of the plane wave pass-by through the reference position by implementing the proposed LWFS approach, with the second row (e-h) depicting the same result with using modal bandlimitation.

The third row illustrates the measured frequency response of the synthesized fields at the reference positions.

The plots reflect that both methods are capable of sufficient suppression of the aliasing wave fronts at the prescribed reference position in a qualitatively similar manner. The frequency responses show that the presented approach slightly suffers from ripples above the spatial aliasing frequency. This remaining aliasing artifact can be explained as the result of the approximations, introduced in the derivation of the spatial-to-temporal filter transform.

In the center position the modal bandlimitation approach serves as a reference solution, with nearly perfect aliasing suppression. For off-center positions both methods suffers from remaining aliasing artifacts. This effect is even enhanced in the case of the front position, in which case the receiver/reference position is closer to the stationary SSD position (white SSD element). The phenomena is explained by the spatial variation of the spatial aliasing frequency and the aliasing intensity, which has been already investigated in details in [4] in a geometrical manner. The incorporation of this effect in the present antialiasing strategy is the subject of further research. Yet, it has been already reported that choosing a non-critical modal bandwidth below the Nyquist wavenumber is an efficient strategy to avoid these remaining aliasing wavefront [7].

V. Conclusion

The present contribution discussed a novel LWFS approach, allowing an increased synthesis accuracy in the proximity of a reference position when a discrete SSD is applied for sound field reproduction. The approach relies on a filter transformation that allows derivation of a temporal filter bank from an arbitrary spatial filter. LWFS is achieved by spatially bandlimiting of the SSD driving function to the Nyquist wavenumber, achieved by suitable spatial filtering. By transforming the spatial antialiasing filters to a temporal filter bank, LWFS can be performed by the simple temporal bandlimitation of the SSD driving signals.

It was demonstrated via numerical simulations that the approach is capable of the suppression of aliasing wavefronts along a straight line/ray, passing through a predefined reference position. The direction of antialiasing synthesis can be set by adjusting the center wavenumber of the antialiasing spatial band-pass filter. The performance of the presented approach was compared with LWFS by direct modal bandlimitation taken as reference solution. It was shown that temporal LWFS gives a feasible approximation for the reference one, while being a more robust approach with less computational demand, allowing real-time implementations. Furthermore, although the proposed approach was validated via the example of a virtual plane wave, the technique is capable of the aliasing-free synthesis of an arbitrary simple virtual field model.

It was demonstrated that both approaches suffer for remaining aliasing artifacts in off-center reference positions. The further mitigation of the off-center aliasing waves is the topic of further research.
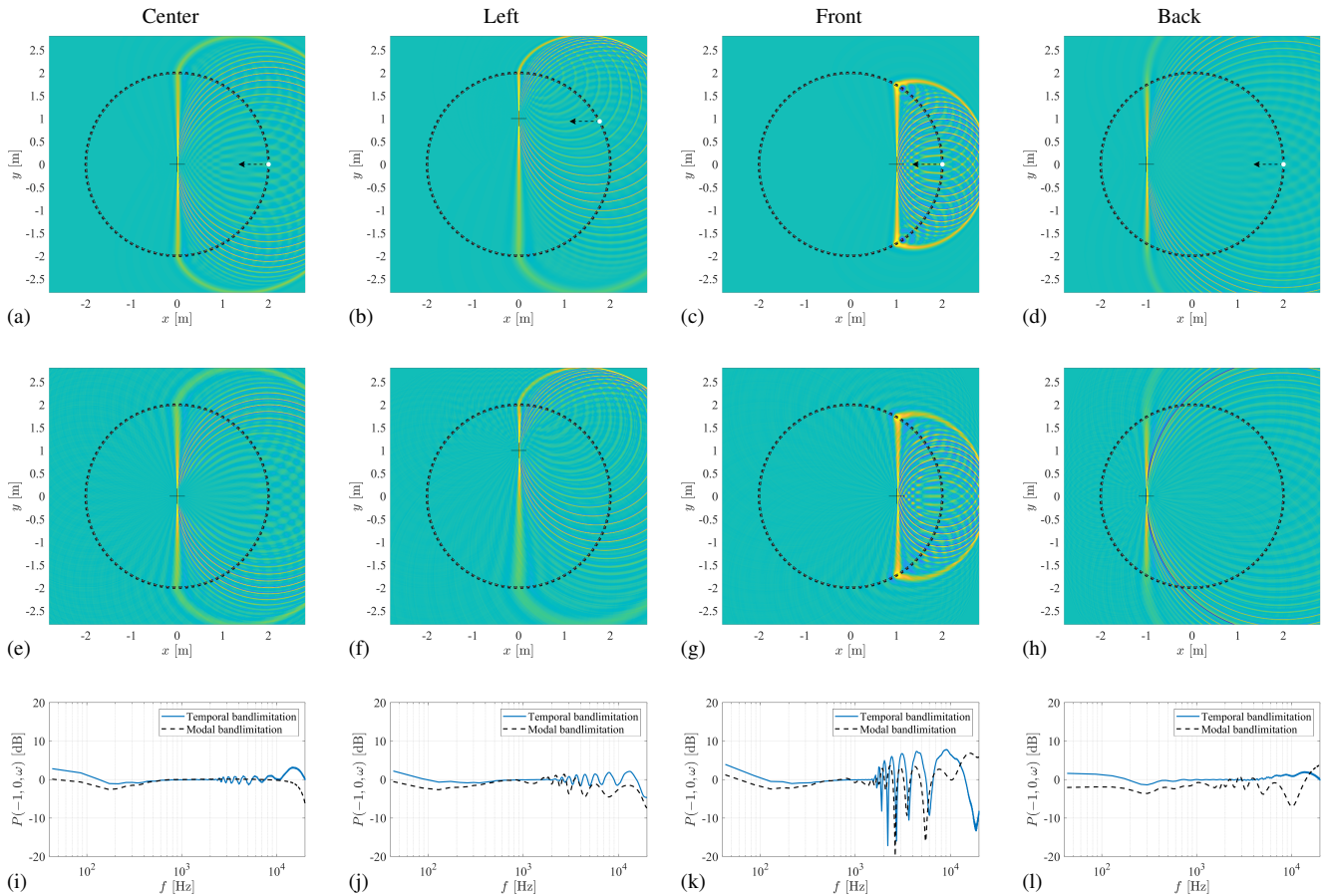
Figure 7. Comparison of the proposed, temporal filtering-based LWFS approach with direct modal bandlimitation. First row (a-d) depicts the synthesized field with temporal LWFS. Second row (e-h) depicts the synthesized field with modal bandlimitation and third row (i-l) compares the frequency response at the reference position.

Finally, as an important limitation of the proposed technique it has to be pointed out, that the proposed approach bandlimits the driving signals as the function of the local propagation direction of the virtual field on the SSD, therefore, the overall synthesis bandlimit varies with the virtual source direction/position. This can result in enhanced artifacts in case of a non-stationary virtual field, e.g. in case of the synthesis of a moving source. The workaround for this phenomena is also the subject of future research.

Acknowledgment

References

[1] A.J. Berkhout, D. de Vries, and P. Vogel. Acoustic control by wave field synthesis. *J. Acoust. Soc. Am.*, 93(5):2764–2778, 1993.

[2] E.W. Start. *Direct sound enhancement by wave field synthesis*. PhD thesis, Delft University of Technology, 1997.

[3] F. Winter, H. Wierstorf, C. Hold, F. Krüger, A. Raake, and S. Spors. Colouration in local wave field synthesis. *IEEE/ACM Transactions on Audio, Speech, and Language Processing*, 26(10):1913–1924, October 2018.

[4] F. Winter, F. Schultz, G. Firtha, and S. Spors. A geometric model for prediction of spatial aliasing in 2.5d sound field synthesis. *IEEE/ACM Transactions on Audio, Speech, and Language Processing*, 27(6):1031–1046, June 2019.

[5] F. Winter, J. Ahrens, and S. Spors. On analytic methods for 2.5-d local sound field synthesis using circular distributions of secondary sources. *IEEE/ACM Transactions on Audio, Speech, and Language Processing*, 24(5):914–926, 2016.

[6] N. Hahn, F. Winter, and S. Spors. Local Wave Field Synthesis by Spatial Band-limitation in the Circular/Spherical Harmonics Domain. In *Audio Engineering Society Convention 140*, Paris, France, June 2016.

[7] N. Hahn, F. Winter, and S. Spors. Synthesis of a Spatially Band-Limited Plane Wave in the Time-Domain using Wave Field Synthesis. In *25th European Signal Processing Conference (EUSIPCO)*, pages 673–677, Kos Island, Greece, August 2017.

[8] N. Hahn, F. Schultz, and S. Spors. Cylindrical radial filter design with application to local wave field synthesis. *J. Audio Eng. Soc*, 70(6):510–525, 2022.

[9] G. Firtha and P. Fiala. An analytic method for transforming spatial filtering of wfs driving functions into temporal filtering. In *DAGA2023*, Hamburg, March 2023.

[10] N. Bleistein, J.K. Cohen, and J.W. Stockwell Jr. *Mathematics of Multidimensional Seismic Imaging, Migration, and Inversion*. Springer, 2000.

[11] G. Firtha, P. Fiala, F. Schultz, and S. Spors. Improved referencing schemes for 2.5d wave field synthesis driving functions. *IEEE/ACM*

Trans. Audio, Speech, Lang. Process., 25(5):1117–1127, May 2017.

[12] N. Bleistein. Two-and-one-half dimensional in-plane wave propagation. *Geophysical Prospecting*, pages 686–703, August 1986.

[13] Rozenn Nicol and Marc Emerit. 3D-Sound Reproduction Over an Extensive Listening Area: A Hybrid Method Derived from Holophony and Ambisonic. In *16th Intl. Audio Eng. Soc. Conf., Rovaniemi, Paper 16-039*, number #16-039, Rovaniemi, 1999.

[14] S. Spors. Extension of an analytic secondary source selection criterion for wave field synthesis. In *Proc. of the 123rd Audio Eng. Soc. Convention*, New York, October 2007.

[15] S.M. Deregowski and S.M. Brown. A theory of acoustic diffractors applied to 2-d models. *Geophysical Prospecting*, 31(2A):293–333, April 1983.

[16] G. Firtha. *A Generalized Wave Field Synthesis Framework with Application for Moving Virtual Sources*. PhD thesis, Budapest University of Technologies and Economics, 2019.

[17] F. Schultz. *Sound Field Synthesis for Line Source Array Applications in Large-Scale Sound Reinforcement*. PhD thesis, University of Rostock, 2016.

[18] John David Jackson. *Classical Electrodynamics*. Wiley, third edition, 1999.